On the structural and optical characteristics of zinc telluride thin films

G. I. RUSU[*], P. PREPELIȚĂ, R. S. RUSU, N. APETROAIE, G. ONICIUC, A. AMARIEI
Faculty of Physics, "Al. I. Cuza" University, 11 Carol I Blvd., R-700506, Romania

Zinc telluride (ZnTe) thin films were prepared by vacuum evaporation of polycrystalline ZnTe onto glass substrates at 300-450K. The films were characterized by X-ray diffraction (XRD) and atomic force microscopy (AFM).The crystalline structure was found to be cubic (zinc blende). The film crystallites are preferentially oriented with (111) planes parallel to the substrates XRD patterns and AFM images have been used to determine the microstructural parameters (crystallite size, lattice parameter) of investigated films.The optical bandgap (E_g=1.95 eV-2.40 eV) determined from absorption spectra indicates direct band-to-band transitions. The effect of the deposition conditions and post-deposition heat treatment on the structural and optical properties has been studied.

1. Introduction

Zinc telluride (ZnTe) thin films are widely used in modern technologies of solid-state devices (light-emitting diodes, solar cells, photodetectors, etc.) because of its excellent characteristics, namely large energy bandgap, low resistivity, high transparency in visible spectral domain, etc. [1-4].

For this compound, there is a very sensitive and complex dependence of film microstructure on preparation method and deposition conditions [5-8].

In this connection, many studies have recently been to establish deposition conditions in order to obtain ZnTe films having a particular crystalline structure and morphology [2-6,9].

In a series of previous papers [8,10,11], we have studied some electronic transport and optical properties of vacuum evaporated ZnTe thin films.

In this paper we extended these investigations by studying the dependence of microstructural and optical properties (transmission and absorption spectra) on the film thickness deposition conditions and post-deposition heat treatment.

2. Experimental procedure

ZnTe thin films were prepared by thermal evaporation under vacuum (p~10^{-5} Torr) of ZnTe polycrystalline powder (99.999% purity), using the quasi-closed volume technique [12,13]. Tungsten boats were used as evaporation sources.

Source temperatures T_{es} were monitored by Pt/Pt-Rh thermocouples which were attached to the bottom of the boats. The values of T_{ev} ranged between 1000 K and 1250 K.

Films were deposited onto glass substrates. A chromel-alumel thermocouple, which monitored substrate temperature, was attached to the front surface of the substrate. The substrate temperature was varied from 300 K to 450 K.

The film thickness was determined by the multiple-beam Fizeau fringe method [14] at reflection of monochromatic light, λ=550 nm. For investigated samples, film thickness ranged between 0.13 μm and 2.80 μm.

The film structure was analysed by X-ray diffraction (XRD) technique (using a DRON-2 diffractometer and CoK$_\alpha$ radiation).

The surface morphology was studied by means of atomic force microscopy (AFM).

The temperature dependence of the electrical conductivity has been studied on surface-type cells [13,15]. Thin indium films were used as electrical ohmic contacts.

The experimental arrangements for study of the electrical conductivity on the temperature are described in our previous papers [8,15-17].

Optical transmission and reflection spectra (in the wavelength range from 300 nm to 1400 nm) were recorded using a double beam spectrometer PMQII (C.Zeiss).

The absorption coefficient, α, was calculated from expression [15,18]

$$\alpha = \frac{1}{d} \ln \frac{(1-R)^2}{T} \qquad (1)$$

Where d is the film thickness, and R and T represent the reflection and transmission coefficient, respectively.

3. Results and discussion

3.1 Structural characteristics

Analysis of XRD patterns (Fig. 1a) indicates that the studied samples are polycrystalline and have a zinc blende (cubic) structure.
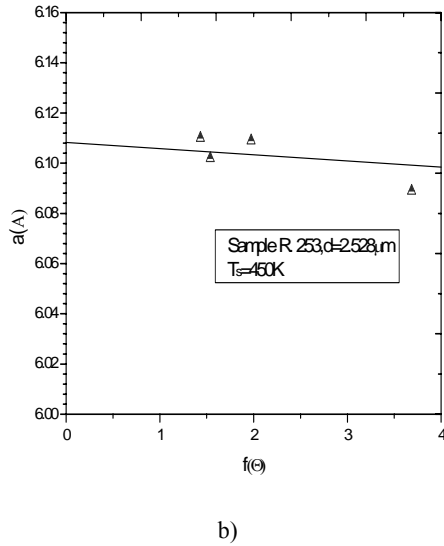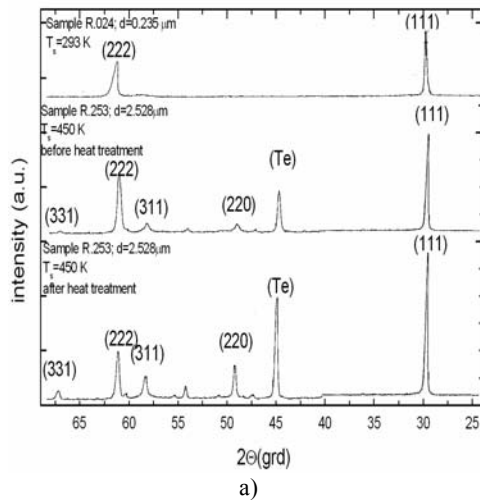
a)

b)

Fig. 1a). XRD patterns for samples R.024 and R.253 b) Nelson-Riley plots for accurate measurement lattice constants of ZnTe thin films.

Different diffraction peaks were identified and the corresponding values of interplanar spacing, d_{hkl} (h,k,l are Milles indices), were calculated from the Bragg equation [19,20]

$$2d_{hkl}\sin\theta = n\lambda \qquad (2)$$

and compared with the standard values [1,2]

The lattice parameter, a, for ZnTe cubic phase structure was determined by the relationship [19]

$$a = d_{hkl}\left(h^2 + k^2 + l^2\right)^{\frac{1}{2}} \qquad (3)$$

The values of the interplanar spacing and cubic lattice parameters are indicated in Table 1. The corrected values of lattice parameter are estimated from Nelson-Riley [19-21] method. Consequently, Nelson-Riley function

$$f(\theta) = \frac{1}{2}\left(\frac{\cos^2\theta}{\sin\theta} + \frac{\cos^2\theta}{\theta}\right) \qquad (4)$$

(where θ is Bragg angle) is calculated and the Nelson-Riley plots are represented for different diffractograms.

In this method the value of lattice parameter is determined by extrapolating of Nelson-Riley functions to $f(\theta) \rightarrow 0$ (Fig. 1b). The obtained values was a=6.142 Å.

Table 1. Structural characteristics of some samples.

Sampled	d (μm)	T_s (K)	(hkl)	2θ (deg)	d_{hkl} (Å)	a (Å)	$\beta_{2\theta}$ (mrad)	D (nm)
R.024	0.235	293	(111)	29.2	3.540	6.089	2.90	57.3
			(222)	60.8	1.766	6.110	7.65	24.4
R.253 B	2.528	450	(111)	29.2	3.540	6.089	3.90	42.2
			(220)	48.9	2.160	6.109	4.25	41.6
			(311)	58.2	1.840	6.102	7.14	25.8
			(222)	60.9	1.766	6.110	5.78	32.3
R.253 A	2.528	450	(111)	29.3	3.540	6.089	3.90	42.6
			(222)	60.9	1.766	6.110	6.63	29.3

(hkl), Miller indices of the planes; d, film thickness; T_s, substrate temperature; $\beta_{2\theta}$ fullwidth at half-maximum of diffraction peaks; D, crystallite size; A, after heat treatment; B, before heat treatment.

The XRD patterns show (Fig. 1a) that the film crystallites are preferentially oriented with (111) planes parallel to the surface substrate (in addition to other prominent reflections (222), (220)).

The high degree orientation is observed for films with smaller thickness (d < 0.4 μm). At greater thickness the orientation of film crystallites is changed.

After a heat treatment (consisting of several successive heating/cooling cycles within the temperature range, ΔT=300-475K [8,10,11,17]), a significant increase of peak intensities, corresponding to (220) and (311) plane take place. For films with greater thickness a characteristic peak for tellurium crystals at about 2θ=45^0 [12] has been observed. We consider that this behavior is due to tellurium excess atoms in the films. These atoms may diffuse at crystallite boundaries and form Te microcrystallites for films with greater thickness. The heat treatment favours this effect (Fig. 1).

The crystallite size, D, was determined using the Debye-Scherrer formula [19-21]

$$D = k\lambda\left(\beta_{2\theta} * \cos\theta\right)^{-1} \qquad (5)$$

where k is the Scherrer constant (k=0.90[19]),λ denotes the wave length of used radiation (for CoKα, λ=1.7889 Å), $\beta_{2\theta}$ is the full-width at half-maximum of the peak considered.

For studied samples, the crystallite size (ranged between 24 nm and 58 nm), increases with increasing film thickness and substrate temperature (from 300 K to 450 K).

For samples with greater thickness (d > 0.4 μm) the heat treatment little influenced crystallite size (Table 1).

a)

b)
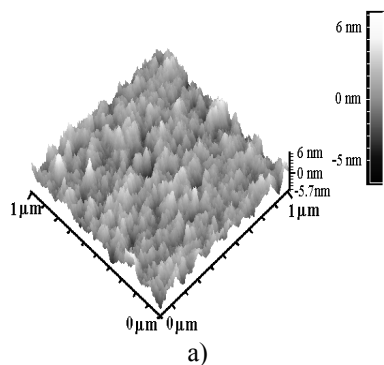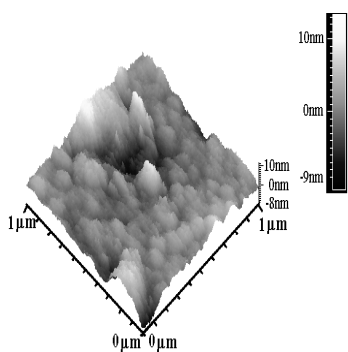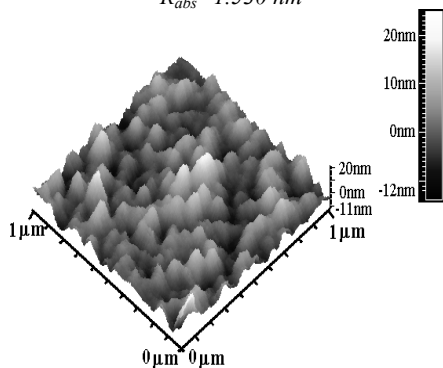
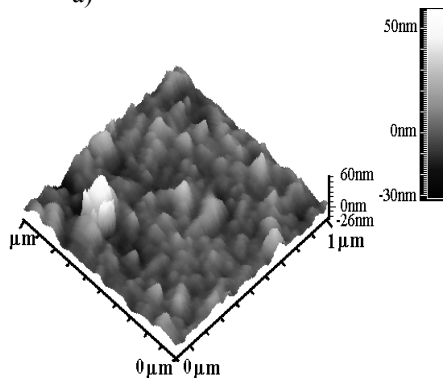*Fig. 2. AFM image (1μm×1μm) for sample S.036 (d=0.358 μm) a) -before heat treatment: R_{rms}=1.405nm; R_{abs}=1.107nm b) -after heat treatment: R_{rms}=1.960nm; R_{abs}=1.530 nm*

a)

b)

Fig. 3. AFM image (1μm×1μm) for sample S.128 (d=1.28 μm), a) -before heat treatment (R_{rms}=4.650nm; R_{abs}=3.680nm), b) -after heat treatment (R_{rms}=9.020nm; R_{abs}=6.230 nm).

Figs. 2 and 3 show the typical AFM images for studied samples. We observe that the films have a grain-like surface morphology. The AFM images provide some quantitative data about the surface roughness and crystallite size of the studied thin forms, as shown in Table 2 and Fig. 4.
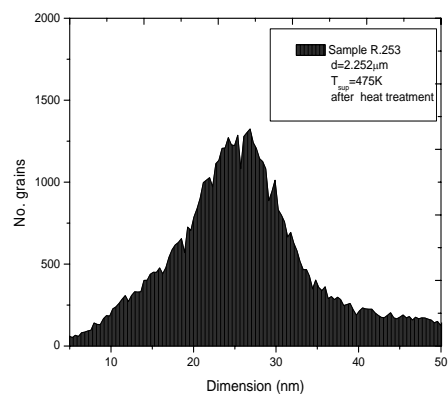
Table 2. Roughness of the film surface.

Sample	d(μm)	T_s(K)	R_{rms}	R_{abs}
T.168	1.697	313	4.06	3.02
T.200	2.000	313	3.69	2.61
T. 052	0.523	298	2.99	2.01
T.075	0.749	298	1.68	1.31
R.026	0.257	313	1.42	1.05
R.253	2.525	473	8.92	5.81

d, the thickness thin films; T_s, the support temperature; R_{abs}, the average roughness and R_{rms}, root mean square roughness.
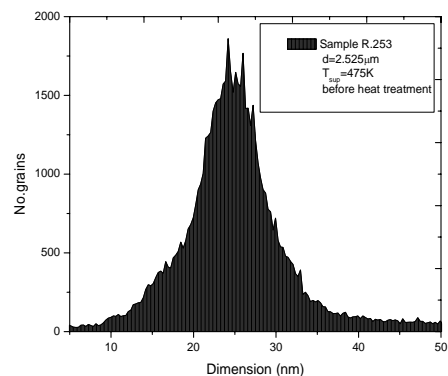
a)

b)

Fig. 4. The histograms sample R.253: a) -before heat treatment; b) -after heat treatment.

The average roughness, R_{abs} increases from 1.05 nm to 5.81 nm and the root mean square roughness, R_{rms}, increases from 1.42 nm to 8.92 nm, when the films thickness increases between 0.257 μm and 2.525 μm.

The crystallite size distribution for two studied samples is represented in Fig. 4.

After heat treatment, the films show an enlargement of the large crystallites and the structure is also strongly densities. This process is accompanied by a reduction of the crystallite high.

3.2 Optical properties

It is known, that in the vast majority of papers studying optical properties of polycrystalline semiconducting films the effect of crystallite boundaries are neglected on the assumption that such influences on the optical properties are usually small [13,15,22].

Relating to optical absorption, it was experimentally established that absorption spectra of the polycrystalline semiconducting films possess an additional absorption peak (compared to single-crystal films) for photon energies less than energy bandgap [22]. This absorption is not important for ZnTe which is a semiconductor compound characterized by direct opticalgap [1-4].

The optical transmission spectra are shown in Fig. 5 for two ZnTe films with different thickness. It can be observed that, generally, the transmission is high which can be attributed to the improvement in structure and stoichiometry of the films. After heat treatment the transmission coefficient strongly decreases (Fig. 6). This effect is due to presence in films of tellurium microcrystallites (this fact is confirmed by XRD patterns), which have a greater absorbance in the visible domain [18,24].
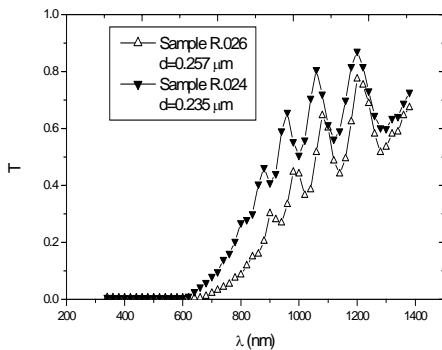

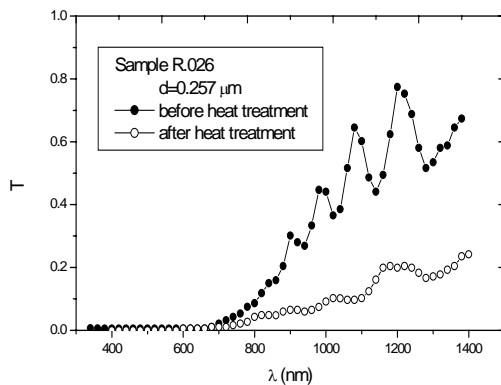Fig. 5. Transmission spectra for samples R.024 and R.026.

Fig. 6. Effect of the heat treatment on the transmission spectra (sample R026).

The estimation of the spectral dependence of absorption coefficient was calculated using a method elaborated by Swanepoel [25,26]. This method (which has been used in a series of our papers [8,10,15,16]) take into account the anvelopes around the interference maxima, T_M, and minima, T_m, due to multiple reflections at the film interfaces.

The shape of the absorption edge is determined by the characteristics of optical interband transitions (Fig. 7) [14,18,22].

For allowed direct transitions (neglecting exciton effects), the energy dependence of the absorption coefficient, α, near the band edge is described by the expression [14,18,22,27]

$$\alpha \cdot h\upsilon = A_a (h\upsilon - E_g)^{1/2} \qquad (6)$$

where $h\upsilon$ is incident photon energy, A_a denotes a characteristic parameter (independent of photon energy) for respective transitions, and E_g is energy bandgap, (at wavevector $\vec{k} = 0$).
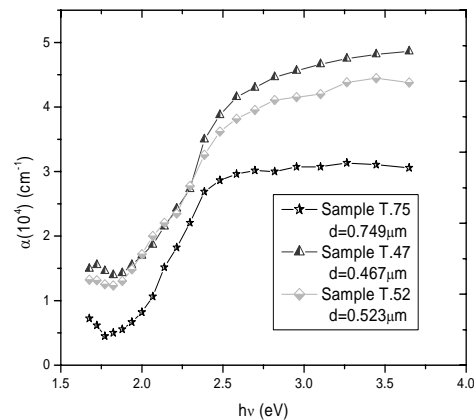

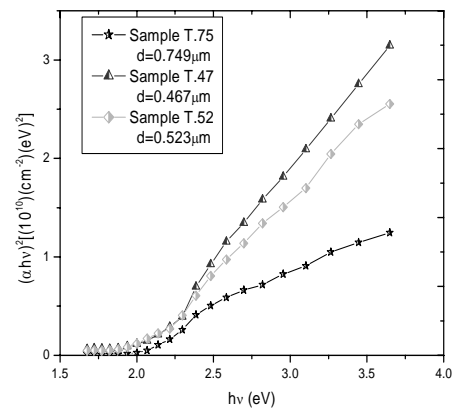Fig. 7. Spectral dependence of absorption coefficient for different ZnTe thin films.

Fig. 8. Dependence $(\alpha h\upsilon)^2 = f(h\upsilon)$ for studied samples.

In vicinity of fundamental absorption edge, according to Eq. (6), the dependence $(\alpha h\upsilon)^2 = f(h\upsilon)$ must be linear. Fig. 8 shows this dependence for three studied samples and confirms the direct nature of band-to-band transitions. The optical energy gap, E_g, was determined by extrapolating the linear portions of $(\alpha h\upsilon)^2 = f(h\upsilon)$ dependences to $(\alpha h\upsilon)^2 = 0$. For studied samples the optical bandgap values ranged between 1.95 eV and 2.40 eV, which are in good agreement with the values of bandgap width reported for ZnTe crystals [1,2,28].

4. Conclusions

A study on the crystalline structure and morphology of vacuum evaporated ZnTe thin films has been made by X-ray diffraction technique and atomic force microscopy. The films are polycrystalline and exhibit a zinc blende structure.

The optical bandgap determined from absorption spectra (supposing allowed direct band-to-band transitions) varied between 1.95 eV and 2.40 eV.

Acknowledgement

Refereces

[1] M. Jain (Ed), II-VI Semiconductor Compounds, World Scientific, Singapore, (1993).
[2] R. Bhargava (Ed), Properties of Wide Bandgap II-VI Semiconductors, Inspec. London (1997).
[3] A. Rohatgi, R. Sudharsanan, S. A. Ringel, Sol.Cells. **27**, 566 (1978).
[4] P. K. Kalita, B. K. Sarma, H. L. Das, Ind. J. Pure and Appl. Phys. **37,** 885 (1999).
[5] A. K. S. Aqili, Z. Ali, A. Mazsood, Appl. Surf. Sci. **167**, 1 (2000).
[6] M. R. H. Khan, J. Phys D Appl. Phys. **27**, 2190 (1994).
[7] W. I. Tao, M. Jurkovic, I. N. Wang, Appl. Phys. Lett. **64,** 1848 (1994).
[8] G. I. Rusu, P. Prepeliţă, N. Apetroaei, G. Popa, J. Optoelectron. Adv. Mater. **7**, 829 (2005).
[9] T. Mahalingam, V. S. John, G. Ravi, P. J. Sebastian, Surf. Coat. Technol. **155**, 245 (2002).
[10] H. Bellakhder, A. Outzourhit, E. L. Ameziane, Thin Solid Films **382**, 20 (2001).
[11] T. Ishizaki, T. Ohmoto, A. Fuwa, J. Phys. D: Appl. Phys. **37**, 255 (2004).
[12] G. G. Rusu, M. Rusu, Solid State Commun. **116**, 363 (2000).
[13] G. I. Rusu, M. E. Popa, G. G. Rusu, I. Salaoru, Appl. Surf. Sci. **218**, 222 (2003).
[14] K. L. Chopra, Thin Film Phenomena, McGraw- Hill, New York(1969).
[15] M. Rusu, I. Salaoru, M. E. Popa, G. I. Rusu, Intern. J. Mod. Phys. **B18**, 1287 (2004).
[16] R. S. Rusu, G. I. Rusu, J. Optoelectron. Adv. Mater **7,** 823, (2005).
[17] G. I. Rusu, I. Caplanus, L. Leontie, A. Airinei, E. Butuc, D. Mardare, I. I. Rusu, Acta.Mater. **49,** 553 (2001).
[18] J. N. Hodgson, Optical Absorption and Dispersion in Solids, Chapman & Hall, London (1970).
[19] B. D. Cullity, Elements of X-ray Diffraction, Addison-Wesley, Reading, Massachusetts **356**, (1979).
[20] P. E. Y. Flewitt, R. K. Wild, Physical Methods for Material Characterization, IOP Publishing Ltd, London, 1994.
[21] N. Tigau, V. Ciupina, G. Prodan, G. I. Rusu, E. Vasile, J. Cryst. Growth, **269,** 392 (2004).
[22] L. L. Kazmerski (Ed), Polycrystalline and Amorphous thin Films and Devices, Academic Press, New York (1980).
[23] C. Baban, Y. Toyoda, M. Ogita, J. Optoelectron. Adv. Mater. **7**, .891, (2005).
[24] M. Rusu, Appl. Phys.A **66**, 357 (1998)
[25] R. Swanepoel, J. Phys. E Sci. Instrum. **16,** 121 (1983); **17**, 896 (1984).
[26] J. C. Manifacier, J. Gasiot, J. P. Fillard, L. Vicario, Thin Solid Films **41**, 127 (1977); **37,** 329 (2002).
[27] K. Seeger, Semiconductor Physics, Springer, Berlin, Heidelberg-New-York, 1999
[28] M. Nishiq, K. Hayashida, Q. Guo, H. Ogawa, Appl. Surf. Sci. **169/170**, 223 (2001).

_____
*Corresponding author: girusu@uaic.ro